

MAGNETORESISTANCE INVESTIGATION OF THE FERMI SURFACE OF MAGNESIUM*

R. W. Stark, T. G. Eck, W. L. Gordon, and F. Moazed
 Department of Physics, Case Institute of Technology, Cleveland, Ohio
 (Received April 5, 1962)

Considerable confusion exists in the literature concerning the interpretation of the magnetoresistance of the hexagonal close-packed metals. This is especially true for magnesium, where the limited data published¹ suggest a Fermi surface topology that is inconsistent with Falicov's band calculation for Mg.² The purpose of this Letter is to summarize the results of a detailed investigation of the transverse magnetoresistance of Mg and to show that these results are in essential agreement with Falicov's Fermi surface (the free-electron surface³ with dimensions adjusted by the band calculation) as modified by Cohen and Falicov to take into account the effects of spin-orbit coupling⁴ and magnetic breakdown.⁵

Alekseevskii *et al.*⁶ and Fawcett⁷ have discussed the behavior to be expected at low temperatures and high magnetic field strengths for the transverse magnetoresistance of high-purity metal single crystals. They conclude that for those magnetic field directions for which all electron trajectories on the Fermi surface are closed, the magnetoresistance increases quadratically with field strength, H , for $V_1 = V_2$ and approaches saturation for $V_1 \neq V_2$. V_1 and V_2 are the "electron" and "hole" volumes defined in reference 6. For those field directions for which there exists a layer of open trajectories with a single average direction, the resistance will have the form $AH^2 \cos^2 \alpha + B$, where A and B are independent of H , and α is the angle between the direction of the current, J , and the direction of the open trajectories. The free-electron Fermi surface³ for Mg predicts quadratic behavior due to $V_1 = V_2$ for most field directions. Thus, the significant directions of H are those for which the transverse magnetoresistance approaches saturation for some or all directions of J .

We have obtained transverse magnetoresistance rotation patterns for a large number of current directions in fields as high as 22 000 gauss. For these rotation patterns the magnetoresistance voltage was continuously recorded as the magnet was slowly rotated (about 20° per minute) in the plane perpendicular to the current by means of a simple friction drive. The residual resistance ratios ($R_{300^\circ\text{K}}/R_{4.2^\circ\text{K}}$) of the crystals investigated varied from 450 to 900 with most of the specimens

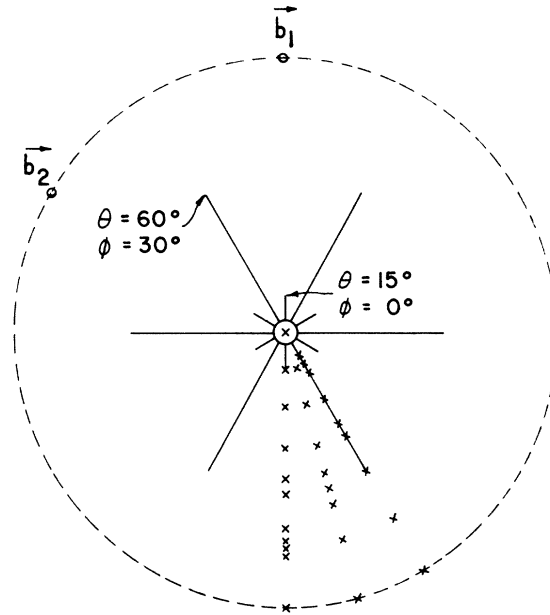


FIG. 1. Stereogram of the significant magnetic field directions for magnesium. b_1 , b_2 , and b_3 are the basis vectors of the hexagonal reciprocal lattice. The pole of the stereogram is along the sixfold b_3 axis. The crosses show the current directions for the specimens investigated.

having the lower value.

Figure 1 is a stereographic projection in reciprocal space of those directions of H for which the transverse magnetoresistance shows evidence of the onset of saturation for at least one direction of J . Directions of H will be given by the coordinates θ , the angle between H and the polar axis b_3 , and ϕ , the angle between the plane of H and b_3 and the plane of b_1 and b_3 . Current directions will be designated by θ' and ϕ' defined in the same manner. For H within the region indicated by the circle about the pole of the stereogram ($\theta \sim 5^\circ$), the transverse magnetoresistance approaches saturation for all directions of J . For H in the directions indicated by the radial lines of Fig. 1, the transverse magnetoresistance shows evidence of saturating for J near the plane of H and b_3 ($\phi' = \phi + 180^\circ$) and approximately quadratic behavior for all other current directions. With the available specimen purity and maximum mag-

netic field strength, it was not possible, for a number of the field directions indicated in Fig. 1, to achieve even an approach to complete saturation of the magnetoresistance. However, for these field directions plots of resistance vs current direction fit quite well a curve of the form $C \cos^2 \alpha + D$, where C and D are constants for a given magnitude and direction of H , and α is the angle between J and the normal to the plane of H and b_3 .

Our results seem to require for their interpretation: (1) all closed orbits with $V_1 \neq V_2$ for H near b_3 , (2) open orbits perpendicular to the plane containing H and b_3 for H in the directions indicated by the radial lines of Fig. 1, and (3) all closed orbits with $V_1 = V_2$ for other directions of H .

Falicov's Fermi surface for Mg consists, in the single zone scheme, of a number of closed surfaces in the first, third, and fourth bands, plus a multiply-connected hole surface in the second band. Only the second band hole surface can give rise to open orbits in the absence of magnetic breakdown. This hole surface is shown in an extended zone scheme in Fig. 1 of reference 7. The connectivity parallel to the hexagonal axis is the result of a small spin-orbit interaction,⁴ the neglect of which would lead to the more familiar double-zone scheme Fermi surface³ that could not support open orbits parallel to b_3 .

We have found no evidence for the presence in Mg of the aa and dd open orbits of reference 7, Fig. 1. The absence of the aa orbits parallel to b_3 is very likely due to magnetic breakdown of the small spin-orbit interaction responsible for the connectivity parallel to b_3 . The dd orbits, which are predicted for Falicov's Fermi surface dimensions² for θ in the range from 71° to 81° and $\phi = 30^\circ, 90^\circ$, etc., would not be present with relatively slight modifications of the dimensions for the "ring" of the second band surface.

Both the open orbits we observe and the region of lack of volume compensation ($V_1 \neq V_2$) can be explained by magnetic breakdown near the basal plane between the second-band hole surface and a portion (the "cigars") of the third-band electron surface. Cohen and Falicov⁵ have used this mechanism to account for the "giant" orbits observed for H near b_3 by Priestley during his de Haas-van Alphen investigation of Mg. The presence of these giant orbits would lead to $V_1 \neq V_2$ over a range of θ in good agreement with our results. Figure 2 shows the projection on the basal plane of two of the types of open orbits we invoke to explain the rest of our data. As H is tilted away

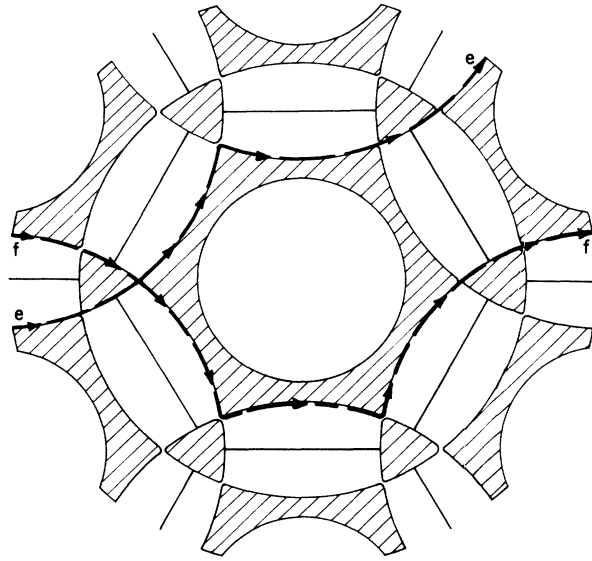


FIG. 2. Open orbits in magnesium. The figure shows a basal plane section of the Fermi surface and a projection on this plane of two of the types of open orbits made possible by magnetic breakdown between the "ring" of the second-band surface and the "cigars" in the third band.

from b_3 in the $\phi = 30^\circ$ plane, one obtains a layer of open orbits that pass through two regions of breakdown, below a region of breakdown, through two regions of breakdown, etc. (ee orbits), and have a net direction perpendicular to the plane containing H and b_3 . Orbits of this type account for the longer of the radial lines of Fig. 1, which extend to a value of $\theta \approx 60^\circ$. Tilting H away from b_3 in the $\phi = 0^\circ$ plane gives rise to the ff open orbits of Fig. 2, which pass alternately through and above two regions of breakdown. These orbits vanish for $\theta \approx 15^\circ$. Using Falicov's dimensions for the ring of the second-band surface and a height for the region of breakdown estimated from the range of H directions for which Priestley sees giant orbits, we predict values of θ for the vanishing of the ee and ff types of open orbits that agree quite well with the values given above. This interpretation of the transverse magnetoresistance data is strongly supported by results we have obtained for the behavior of the transverse-even and Hall voltages in Mg.

We wish to thank B. W. Roberts for generously supplying most of the magnesium crystals used in this work and L. Falicov for many stimulating discussions.

*This work has been supported by the Air Force Office of Scientific Research.

¹N. E. Alekseevskii and Yu. P. Gaidukov, *J. Exptl. Theoret. Phys. (U.S.S.R.)* **38**, 1720 (1960) [translation: *Soviet Phys. - JETP* **11**, 1242 (1960)].

²L. M. Falicov, thesis submitted to the University of Cambridge, England, 1960 (unpublished); and to be published.

³W. A. Harrison, *Phys. Rev.* **118**, 1190 (1960).

⁴M. H. Cohen and L. M. Falicov, *Phys. Rev. Let-*

ters **5**, 544 (1960).

⁵M. H. Cohen and L. M. Falicov, *Phys. Rev. Let-*

ters **7**, 231 (1961).
⁶N. E. Alekseevskii, Yu. P. Gaidukov, I. M. Lifshitz, and V. G. Peschanskii, *J. Exptl. Theoret. Phys. (U.S.S.R.)* **39**, 1201 (1960) [translation: *Soviet Phys. - JETP* **12**, 837 (1961)].

⁷E. Fawcett, *Phys. Rev. Letters* **6**, 534 (1961).

ELECTRON NUCLEAR DOUBLE RESONANCE STUDY OF LITHIUM A CENTERS IN KCl[†]

Robert Lee Mieher*

II. Physikalisches Institut der Technischen Hochschule, Stuttgart, Germany

(Received April 2, 1962)

Optical studies¹⁻³ on KCl have shown a relation between the optical absorption band at 589 m μ , the A band, and the sodium impurity content of the crystal. The A centers are present after short illumination times of the F centers in a freshly quenched crystal. Studies with polarized light have shown that the A centers can be polarized in a [100] direction and have a second optical absorption band under the F band. It has been proposed¹⁻³ that the A center is an F center associated with a Na ion in one of the six nearest neighbor positions. This Letter reports an optical study of a similar center in which the F center is associated with a lithium³ impurity and an electron nuclear double resonance (ENDOR) study that verifies the general A-center model of an F center associated with an alkali impurity.

Figure 1 shows the optical absorption bands that result when a KCl crystal is grown with 1% LiCl in the melt and then additively colored to a concentration of 3×10^{17} F centers/cc. Curve 1 of Fig. 1(a) is the F-center absorption band that is present after the crystal is quenched from 650°C to room temperature and then measured at -180°C (all measurements were made at liquid O₂ temperature). Curve 2 of Fig. 1(a) is obtained after five minutes exposure at room temperature to green light centered at 546 m μ . The effects of polarizing the A centers with 546-m μ light polarized along a [100] direction is shown in Fig. 1(b). Curve 1 is obtained with [010] polarized measuring light and curve 2 with [100] light.

If the axis of the A center is taken to be the line from the vacancy to the impurity, then the A₂ band is excited by light with electric vector perpendicular to the axis of the center and the A₁ band is excited by light with electric vector parallel to

the axis (see reference 1 for a general discussion). Table I compares the peak positions of the optical absorption bands in KCl containing Na to those in KCl containing Li.

The results of an ENDOR study of the lithium A center are shown in Fig. 2. The meaning of the notation above the ENDOR line is as follows: The +, - superscripts indicate the state of the electron, $m_S = \pm \frac{1}{2}$; the \parallel , \perp subscripts indicate the angle between the magnetic field and a line from the vacancy to a given nucleus; the K _{α} nucleus is the single potassium opposite the lithium, i.e., on the axis of the center, and the K _{β} nuclei are the four potassiums located in the plane perpendicular to the axis of the A center.

The ENDOR spectrum of the nearest neighbor potassium nuclei of the F center in a quenched crystal is shown in Fig. 2(a). After an optical treatment similar to that used to produce curve 2 of Fig. 1(a), the ENDOR spectrum appears as given in Fig. 2(b). One interesting feature is the K _{α} \parallel ⁻ quadrupole triplet which consists of three sharp lines. They are about one-half as high as the K _{β} \parallel ⁻ lines although there are only one-fourth as many K _{α} nuclei as K _{β} nuclei. The explanation is that the K _{α} nucleus is opposite the Li and, therefore, has no equivalent nucleus to produce the second order hyperfine interaction⁴⁻⁶ that gives the additional fine structure to the K _{β} \parallel ⁻ quadrupole triplet. This explanation is verified in Figs. 2(c) and 2(d). In Fig. 2(c) the A centers have been polarized with their axes parallel to the magnetic field and there are strong K _{α} \parallel ⁻ and Li \parallel ⁻ lines present with very weak K _{β} \parallel ⁻ and Li \perp ⁻ lines. In Fig. 2(d) the crystal has been rotated 90° and the centers are then perpendicular to the field. The relative intensities are just re-